Available online at www.sciencedirect.com
SCIENCE DIRECT
Biochimica et Biophysica Acta 1708 (2005) 311 – 321
BIOCHIMICA ET BIOPHYSICA ACTA
BBA
http://www.elsevier.com/locate/bba

Photosynthetic activity of far-red light in green plants

Hugo Pettai[a], Vello Oja[a], Arvi Freiberg[a,b], Agu Laisk[a,*]

[a]*Institute of Molecular and Cell Biology, University of Tartu, Riia Street 23, Tartu, 51010, Estonia*
[b]*Institute of Physics, University of Tartu, Riia Street 142, Tartu 51014, Estonia*

Received 19 August 2004; received in revised form 9 May 2005; accepted 10 May 2005
Available online 23 May 2005

Abstract

We have found that long-wavelength quanta up to 780 nm support oxygen evolution from the leaves of sunflower and bean. The far-red light excitations are supporting the photochemical activity of photosystem II, as is indicated by the increased chlorophyll fluorescence in response to the reduction of the photosystem II primary electron acceptor, Q_A. The results also demonstrate that the far-red photosystem II excitations are susceptible to non-photochemical quenching, although less than the red excitations. Uphill activation energies of 9.8 ± 0.5 kJ mol^{-1} and 12.5 ± 0.7 kJ mol^{-1} have been revealed in sunflower leaves for the 716 and 740 nm illumination, respectively, from the temperature dependencies of quantum yields, comparable to the corresponding energy gaps of 8.8 and 14.3 kJ mol^{-1} between the 716 and 680 nm, and the 740 and 680 nm light quanta. Similarly, the non-photochemical quenching of far-red excitations is facilitated by temperature confirming thermal activation of the far-red quanta to the photosystem II core. The observations are discussed in terms of as yet undisclosed far-red forms of chlorophyll in the photosystem II antenna, reversed (uphill) spill-over of excitation from photosystem I antenna to the photosystem II antenna, as well as absorption from thermally populated vibrational sub-levels of photosystem II chlorophylls in the ground electronic state. From these three interpretations, our analysis favours the first one, i.e., the presence in intact plant leaves of a small number of far-red chlorophylls of photosystem II. Based on analogy with the well-known far-red spectral forms in photosystem I, it is likely that some kind of strongly coupled chlorophyll dimers/aggregates are involved. The similarity of the result for sunflower and bean proves that both the extreme long-wavelength oxygen evolution and the local quantum yield maximum are general properties of the plants.

Keywords: Quantum yield of photosynthesis; O_2 evolution; Photosystem II; Far-red chlorophyll

1. Introduction

The quantum yield of photosynthesis, calculated per absorbed light quanta, drops at the red end of the absorption spectrum of leaves and green algae [1,2]. This drop can be compensated with the help of an accompanying illumination at shorter wavelengths, a phenomenon known as Emerson enhancement effect [3]. The reason of the red drop is the unequal distribution of excitations between the two photosystems, photosystem II (PSII) and photosystem I (PSI), which operate as a tandem [4]. For stable operation with high efficiency, electron transport rates through the two photosystems must be closely equal that requires similar excitation rates. The antenna system of PSI contains a number of so-called far-red chlorophylls (Chls), which absorb at wavelengths beyond 700 nm [5]. As a result, the far-red light is mainly absorbed by PSI. Since the rate of electron donation to PSI is determined by PSII, which is insufficiently excited, it strictly limits the overall quantum yield of photosynthesis at the far-red end of the Chl absorption spectrum. Occurrence of similar far-red Chls in the PSII antenna is not recognized, though O_2 evolution at

Abbreviations: CP, chlorophyll protein; F_0, F_m, chlorophyll fluorescence yield, minimum with open reaction centres and maximum with closed reaction centres; FWHM, full width at half maximum; LED, light-emitting diode; LHC, light-harvesting complex; PSI, PSII, photosystem I and II; PQ, plastoquinone; P680, PSII reaction centre pigment; Q_A, PSII primary acceptor quinone; $Y(\lambda)$, quantum yield of electron transport at wavelength λ

* Corresponding author. Fax: +372 7366 021.
E-mail address: agu.laisk@ut.ee (A. Laisk).

0005-2728/$ - see front matter © 2005 Elsevier B.V. All rights reserved.
doi:10.1016/j.bbabio.2005.05.005

wavelengths beyond 700 nm has been reported [4] and the optical cross-section of the responsible Chls has been calculated [6]. Since this cross-section was very small at 723 nm, it was assumed to be a tail of the Chl a absorption.

Though the red drop has frequently been discussed in earlier photosynthesis research [4,7–9], the extension of oxygen evolution to the far-red end of the spectrum was seldom emphasized [4,6]. After the zirconium-based oxygen analyzer was taken into the armament by photosynthesis researchers [10], precise measurements of O_2 evolution became possible from leaves. Applying the zirconium analyzer for O_2 evolution measurements and a tuneable laser for illuminating the leaves, we are revisiting this classical problem. A distinctive aspect of our approach is that leaves attached to the growing plant are used in the experiments in order to avoid changes that may occur upon disruption of leafs or cells. This way, the light-activated O_2 evolution from sunflower leaves at extraordinarily far-red wavelengths up to 780 nm has been measured [11]. The quantum yield of O_2 evolution has a local peak at 745 nm almost reaching 20% of the maximum yield of 0.39 at 650 nm excitation.

In this work, a more detailed mechanistic investigation of the observations on sunflower leaves has been undertaken by measuring time responses of O_2 evolution rate and fluorescence yield on rapid on/off switching of illumination as well as by evaluating the distribution of excitation between the PSI and PSII complexes. The latter studies involve aspects of non-photochemical quenching (NPQ) of electronic excitations in PSII. We also expanded the investigation to another plant (bean) to check the generality of the observed phenomena.

2. Materials and methods

2.1. Plant material

Sunflower (*Helianthus annuus* L.) and bean (*Phaseolus vulgaris* L.) plants were grown in a growth chamber in 4-l pots in fertilized peat–soil mixture at 25/20° and a 16/8 h day/night regime. The incident photosynthetic photon flux density on the top of the plants was 350 μmol quanta m^{-2} s^{-1}. Fully expanded leaves attached to the plant were used in the experiments. All the measurements, except when specifically noted, were performed using low excitation intensities to avoid light saturation effects.

2.2. Oxygen evolution measurements

A part of a leaf was enclosed in a sandwich-type leaf chamber (diameter 31 mm, thickness 3 mm). To stabilize the leaf temperature at 22 °C, the upper epidermis of the leaf was sealed to the thermostatted glass window with starch gel. The leaf was illuminated from the upper side through the water jacket and the window, while the gas exchange took place through the lower epidermis. The necessary CO_2 concentration of 360 μmol mol^{-1} and O_2 concentration of 210 mmol mol^{-1} (complemented by N_2) were provided by mixing pure gases at stabilized flow rates, the overall gas flow rate being 0.5 mmol s^{-1}. The O_2 evolution rate was measured with a Zr-oxide analyzer Ametek S-3 A (Thermox, Pittsburgh, PA, USA). Low O_2 evolution rates were measured under the background O_2 concentration reduced to 50 μmol mol^{-1} for no longer than 10 min, which was not harmful for the leaf. The two-channel gas flow system (Fast-Est, Tartu, Estonia) ensured fast changes in the O_2 concentration. The water vapour pressure deficit was held at 1.7 kPa.

2.3. Quantum yield measurements

The leaf chamber was illuminated through a multi-armed fibre-optics cable (Fast-Est, Tartu, Estonia). A 650-nm LED light source (Fast-Est, Tartu, Estonia) was used for preconditioning the leaf photosynthesis and stabilization of stomatal opening. A continuous-wave Ti/Sapphire solid state laser (Model 3900S, Spectra Physics, Mountain View, CA, USA) with line width of 0.03 nm was used for the quantum yield measurements at the far-red light wavelengths beyond 700 nm, while a dye laser (Model 375, Spectra Physics, Mountain View, CA, USA) was used at the red-light wavelengths between 650 and 700 nm. The laser beam was guided to the front of the fibre bundle with mirrors and expanded with a lens so that the leaf chamber was illuminated uniformly. An electronically controlled shutter (Fast-Est, Tartu, Estonia) switched the beam on/off with 1.3 ms full front edge. In separate measurements, a constant-wavelength far-red excitation at 716 and 740 nm was applied using an incandescent lamp (KL 1500 from H. Walz, Effeltrich, Germany) in combination with 10 nm FWHM bypass interference filters (Andover Corp. Salem, MA, USA).

The quantum yield of the PSII electron transport, $Y(\lambda)$, with respect to the absorbed quanta at wavelength λ was calculated from the measured rate of oxygen evolution as follows

$$Y(\lambda) = \frac{4A_{O_2}}{I(\lambda)a(\lambda)}, \quad (1)$$

where A_{O_2} is the O_2 evolution rate in μmol m^{-2} s^{-1}, $I(\lambda)$ is the incident photon flux density of the laser beam in μmol m^{-2} s^{-1} and $a(\lambda)$ is the absorptance ranging from 0 to 1, i.e., the ratio of the radiation absorbed by the leaf to the total incident radiation. The multiplier 4 is the number of light-driven one-electron oxidation steps required to oxidize water to molecular oxygen. The incident quantum flux density was measured using a bolometric sensor with even spectral response. The bolometer was calibrated against a LI 190 SB quantum sensor (LiCor, Lincoln, NE, USA) in white light between 400 and 700 nm [12]. During the calibration, both the bolometer and the

quantum sensor were placed in the leaf chamber at the position of the leaf. When the leaf was in the chamber, the light intensity was recorded by a photodiode from a separate bundle of the fibre optics. Care was taken in all measurements to keep the incident light intensity on the linear section of the light response curve.

When one is dealing with a high intensity of very weakly absorbed light, even a tiny amount of stray light that is well absorbed can have a dramatic effect. The critical stray light level with respect to the excitation intensity determined by the sensitivity and dynamic range of our apparatus for O_2 evolution measurements was about 10^{-3}. At the same time, the background illumination intensity of the laser relative to its peak intensity measured 20 nm away from the centre wavelength was less than 10^{-5}. Therefore, excitation via the laser background can be excluded and the below-reported long-wavelength O_2 evolution was caused by the laser emission.

2.4. Leaf absorptance and chlorophyll fluorescence measurements

The leaf absorptance spectrum was measured with a spectral resolution of 3.2 nm in an integrating sphere using a CCD spectro-radiometer PS-2000 (Ocean Optics, Dunedin, FL, USA). A 15.6-mm diameter disk was punched from the leaf and placed in the centre of an 80-mm integrating sphere, made of compressed white Teflon powder (8 mm layer, painted white outside). The disk was illuminated by an incandescent source through a long-pass filter and a single 1-mm plastic fibre. The filter cut off wavelengths shorter than 690 nm, avoiding Chl fluorescence that could interfere with the absorptance measurements at longer wavelengths. For comparative measurements, a white and a black object of similar size replaced the leaf in the direct beam, but the leaf disk was left nearby in the sphere in scattered light. However, the signal level obtained with the white object was used only as an indicator of the correct setup of the sphere. The actual reference level corresponding to zero absorption in chlorophyll was assumed to be that measured with the same leaf disk at 800 nm. Since during the quantum yield measurements, the leaf was sealed to the chamber window with starch paste, we simulated this optical path also in the sphere. The absorptance of the leaf and the layer of starch paste under a glass disk was relatively greater by 2% than the absorptance of the leaf, but the effect did not depend on wavelength between 720 and 760 nm. The corresponding correction factor was applied when leaf disks were measured without the starch paste in the sphere. We also checked whether the absence of O_2 could influence on leaf absorption in the far-red, but no difference was observed when the sphere was flushed with N_2 for 10 min.

The Chl fluorescence at room temperature was measured with the pulse-modulated Chl fluorometer PAM 101 (H. Walz, Effeltrich, Germany). At 1.6 kHz pulsing frequency, the average intensity of the 650-nm excitation beam was low enough not to cause appreciable reduction of Q_A, the primary electron acceptor of PSII. The signals were recorded with a computer using a 12-bit A/D converter board ADIO 1600 (Kontron, San Diego, CA) and a system-operating program RECO (Fast-Est, Tartu, Estonia).

3. Results

3.1. Efficiency of the far-red quanta relative to the photosystem II electron transport

In leaves, the PSII activity was characterized as the photosynthetic O_2 evolution. Before the measurements, the leaf was preconditioned for 20 min in the chamber under illumination with 650-nm red light (flux density of 200 μmol quanta m^{-2} s^{-1}) and 720-nm far-red light (70 μmol quanta m^{-2} s^{-1}). The chamber was flushed with a mixture of O_2 and CO_2 in N_2: 210 mmol mol^{-1} of O_2 and 360 μmol mol^{-1} CO_2. For the O_2 evolution measurements, the background O_2 concentration was rapidly decreased to 50 μmol mol^{-1}, while maintaining the CO_2 concentration, and the preconditioning light sources were exchanged for the laser illumination. The measurements were performed at several pre-set wavelengths between 650 and 790 nm. The reference level (zero O_2 evolution) was determined in the dark, for which the illumination was shuttered off (at such low O_2 concentration the respiratory O_2 uptake is known to be negligible). An example of such measurements is shown in Fig. 1. As one might anticipate, the light-induced O_2 evolution rate decreased rapidly toward longer wavelengths. The rate, however, remained clearly distinguishable above the noise level up to 780 nm.

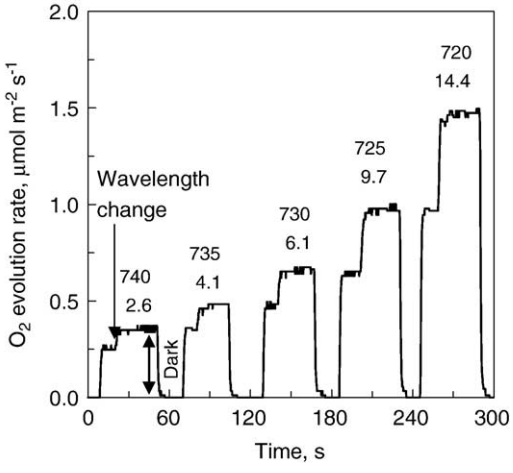

Fig. 1. Oxygen evolution rate traces measured on a sunflower leaf under laser illumination. The laser wavelengths in nm and absorbed light intensities in μmol m^{-2} s^{-1} units are indicated, as is the decrease of the wavelength during exposures. The leaf temperature was 22 °C; the background concentrations of CO_2 and O_2 were, correspondingly, 360 and 50 μmol mol^{-1}. A double-headed arrow specifies the reading taken at 740 nm as an example. The light-saturated O_2 evolution rate of the leaf was 20 μmol m^{-2} s^{-1}.

The quantum yields of PSII electron transport relative to incident (Fig. 2A) and absorbed (Fig. 2B) light were calculated from the measured O_2 evolution rates using the leaf absorptance spectrum. The yield with respect to the incident light rapidly decreased toward longer wavelengths beginning from about 685 nm. However, the yield relative to the absorbed light calculated according to Eq. (1) initially declined from 0.33 at 650 nm to 0.05 at 720 nm, then the trend reversed, until the final drop began at 750 nm (Fig. 2B). This way, a local yield maximum of about 0.07 at 745 nm was formed, while the signal became undetectable at 770 nm in this leaf.

3.2. Oxygen evolution under the far-red light is due to the photosystem II excitation

In order to prove that the observed O_2 evolution was the result of the PSII activity under the far-red light, we measured the time response of the Chl fluorescence to the far-red illumination (Fig. 3). The leaf was pre-adapted in the dark with the aim to inactivate the CO_2 reduction enzymes. Upon the low-intensity 650 nm light switched on at zero time, an initial transient peak in O_2 evolution was recorded, which indicated the process of reduction of plastoquinone (PQ) [13]. The O_2 evolution decreased again when PQ became more reduced, but the CO_2 reduction was not yet activated. The Chl fluorescence transient that started at time = 0 s supports this interpretation showing an increased Q_A reduction after the peak of the O_2 evolution. Similar, although slower, transients of O_2 evolution and Chl fluorescence followed illumination of the dark-adapted leaf with the far-red light.

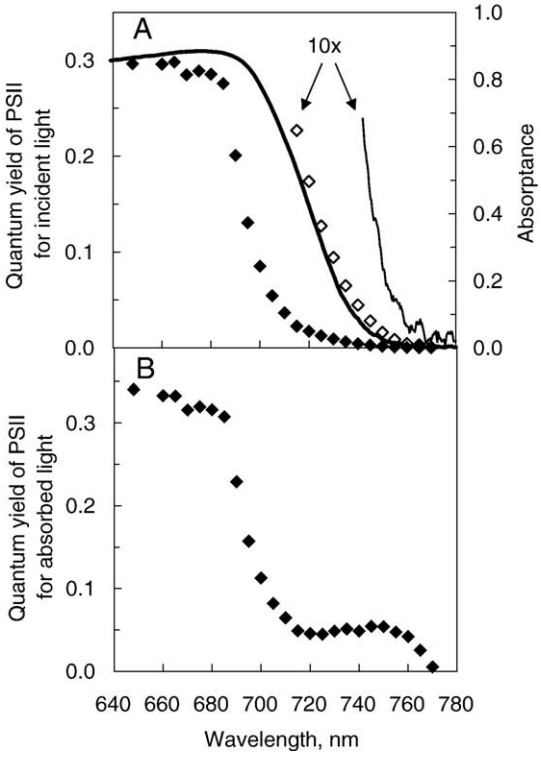

Fig. 2. Wavelength dependence of the quantum yield of photosystem II electron transport calculated from the measured oxygen evolution rate from a single sunflower leaf. Panel A: quantum yield for the incident light (filled diamonds, left ordinate) and the leaf absorptance (thick line, right ordinate). For open diamonds and thin line, the ordinates are increased 10 times. Panel B: quantum yield of PSII electron transport for the absorbed light.

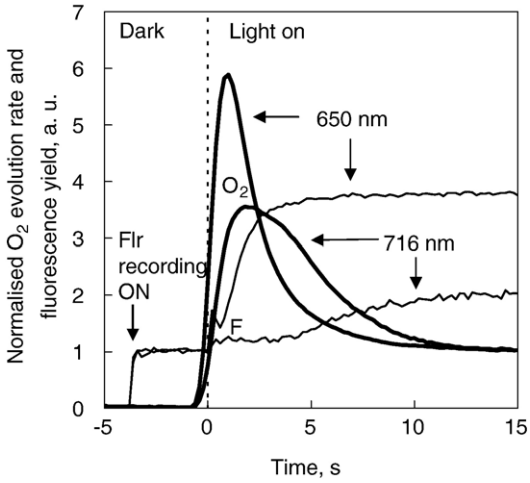

Fig. 3. Oxygen evolution rates (O_2, thick lines) and chlorophyll fluorescence (F, thin lines) transients in a sunflower leaf under 650 and 716 nm excitation. The former are normalized to the steady-state (final) rate and the latter to F_0 (initial) level. The light intensities (incident/absorbed in μmol quanta m^{-2} s^{-1}) switched on at zero time were 31/27 at 650 nm and 120/57 at 716 nm. A weak fluorescence measuring beam at 650 nm was turned on at −3 s.

These results show that the effect of the far-red light is comparable to the effect of the red light. They both excite PSII antenna and cause the reduction of PQ. Note, however, from Fig. 3 that the 716 nm light is almost six times less efficient compared with the 650 nm light, in perfect agreement with [6]. This is because of the very different cross sections for oxygen evolution at these two wavelengths.

3.3. State transition, not spill-over, balances PSII and PSI excitation

For the maximum quantum yield of photosynthesis, excitation must be distributed about equally between the two photosystems. Excitation distribution is determined by the number of Chls (total antenna size) and spectral properties of Chls. State transitions control the distribution of Chls between the photosystems, being able to balance the excitation of the two photosystems at wavelengths of 680 nm and shorter. Spill-over of excitation from the PSII antenna to the PSI antenna is another mechanism that may serve to balance excitation between the photosystems. While the re-distribution of LHC units between the photosystems is a relatively slow process, spill-over is instantaneous. In the following experiment, we used the speed of the transient to reveal which of the two mechanisms – spill-

over or state transition – is responsible for excitation balancing between the photosystems.

Traces of O_2 evolution and Chl fluorescence during the measurement cycle are shown in Fig. 4. The O_2 evolution rate stabilized rapidly after the 716 nm light was turned on at 10 s. Under the far-red light, the PSI was overexcited and the O_2 evolution was limited by the flux of quanta hitting PSII. The rate further increased after the 650-nm light was added to the 716-nm light. Adding the red light to the far-red increased the PSII excitation rate, but PSI still remained either over-excited or exactly balanced with PSII, as indicated by the low fluorescence yield. Thus, the increase in the O_2 evolution rate characterized the true quantum yield of PSII in the 650 nm light.

The long dark pre-exposure plus the following excess excitation of PSI by the 716 nm far-red light shifted the antenna system into state 1, where the mobile LHC units were connected with PSII. When the far-red light was turned off, there was an immediate drop in the O_2 evolution rate, corresponding to the loss of PSII excitation by the far-red light. The rapid drop was followed by a slow decrease of O_2 evolution, accompanied by increasing Chl fluorescence from the previous low (about F_0) level. This indicated Q_A reduction, implying that under the 650 nm light only, PSII was clearly overexcited compared with PSI and the quantum yield of PSII decreased, due to Q_A reduction, to the level that matched PSI excitation. This result could be interpreted as evidence for the lack of fast balancing of excitation between the two photosystems by instant spill-over from the PSII to the PSI antenna, however, we do not know whether spill-over accompanied the increasing fluorescence or not. If it did, then the balancing of the two photosystems occurred, first, due to the decreased PSII yield (reflected by increased fluorescence), and, second, due to the increased PSI excitation due to the enhanced spill-over. However, after the leaf was exposed under the 650-nm light for the following 10 min, the fluorescence yield decreased almost back to the previous F_0 level (Fig. 4B). This slow change can be interpreted only as the state 1→ state 2 transition, during which the PSII antenna decreased to match the PSI antenna (the final increase in F_0 was caused by the long anaerobic exposure; in experiments where the state 1→ state 2 transition was induced in the presence of oxygen, F_0 did not increase, but it was not possible to demonstrate the recording of O_2 evolution). Thus, though this experiment does not rule out the possibility that spill-over was active during the initial phase of the transient, it still confirms the contemporary dominant view that state transitions and not spill-over is the basic mechanism to balance PSII and PSI excitation during steady-state photosynthesis.

3.4. Measurement of the true PSII quantum yield

As one can estimate from Fig. 4 (double arrow at 70 s), the loss of the quantum yield due to the misbalance toward over-excitation of PSII was about 25% in this leaf, indicating that the mobile Chl formed about 12.5% of the total. This implies that the true quantum yield of PSII in the red spectral region can only be measured when the far-red light is added. Without the latter, the quantum yield may be partially limited by PSI excitation, dependent on the state of antenna balancing. This explains why the laser-illuminated PSII quantum yield at 650 nm, without additional far-red excitation, was only 0.33 in the experiment of Fig. 2B. The correctly measured quantum yield averaged over all leaves studied was equal to 0.39 ± 0.03 (Fig. 5). The expected result is 0.4, if a half of the quanta are absorbed in the PSII antenna and 20% PSII excitations are lost before trapping, as indicated by the typical variable fluorescence F_v/F_m of 0.8.

The average quantum yield and absorptance data for ten explored sunflower leaves are presented in Fig. 5A and the

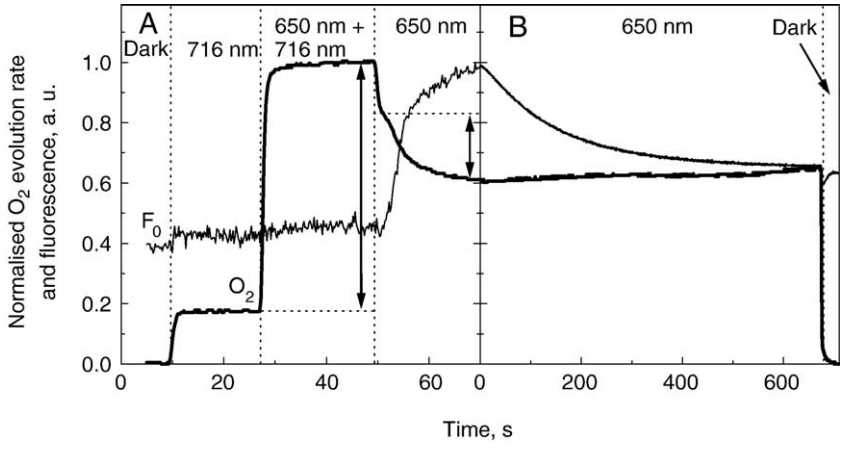

Fig. 4. Oxygen evolution rates (O_2) and chlorophyll fluorescence (F) transients of a sunflower leaf under combined red and far-red excitation. Panel A: at 10 s, the 716 nm excitation was switched on. After 17 s, the 650-nm light was added. Then at 49 s, the 716-nm source was turned off. The O_2 evolution rate difference used to calculate the true quantum yield of PSII for the 650 nm excitation is indicated by the longer double-headed arrow. The shorter arrow indicates quantum yield drop due to PSII over-excitation. Panel B: transients in Chl fluorescence and O_2 evolution due to state 1→ state 2 transition. Light intensities were the same as in Fig. 3.

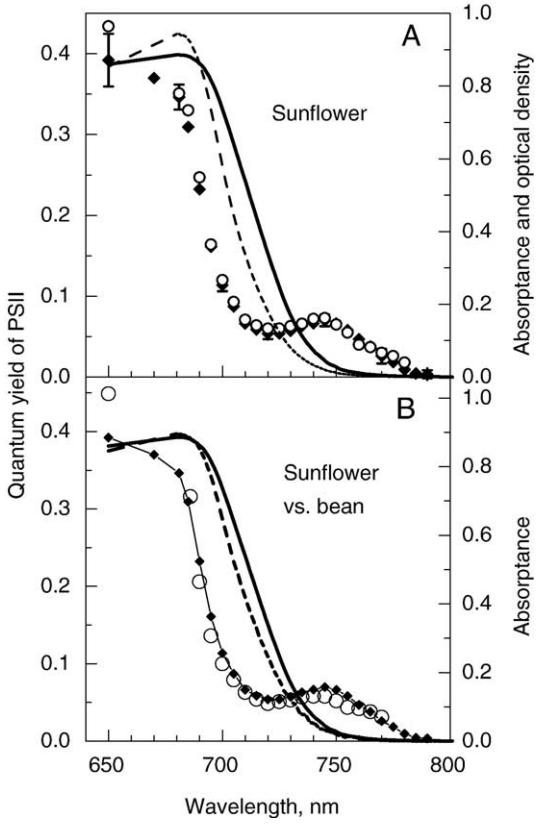

Fig. 5. The spectral dependence of quantum yields of the photosystem II electron transport (left axis, symbols) and absorptance/optical density spectra (right axis, lines) of sunflower and bean leaves. Thick continuous lines in panels A and B represent the absorptance of sunflower leaves, while that for the bean in panel B is shown with dashed line. The thin dashed line in panel A represents the optical density of sunflower leaves. The quantum yield data for sunflower (filled diamonds) is averaged over the ten leaves studied (standard deviation is indicated). In measurements represented by empty circles, the laser beam was attenuated by half compared to the filled diamonds. For bean, the quantum yield data for a single leaf is presented (circles).

same data are compared with those for the bean leaf in Fig. 5B. In sunflower, the scattering of the quantum yield measurements was small, clearly revealing the presence of the local maximum at 745 nm. Empty circles in Fig. 5A represent quantum yield measurements where the laser beam was attenuated by half compared with the filled data points. The obtained equal quantum yield values independent of the beam intensity rule out possible non-linearities in the light dependence of O_2 evolution (e.g. [14]), since the reduction of interphotosystem electron carriers was prevented by continuous PSI overexcitation in our experiments. Though the absorptance of the bean leaf decreased much faster toward longer wavelength compared to sunflower, only minor difference of the quantum yield data is observed between the two species. This result proves that both the extreme long-wavelength O_2 evolution and the local quantum yield maximum are general properties of plants, not just peculiar characteristics of the sunflower leaves.

3.5. Temperature dependence of the photosystem II quantum yield under far-red light

Since the O_2 evolution is a result of the PSII activity and the 680 nm reaction centre is responsible for the photochemistry, the far-red light-supported O_2 evolution should be an uphill process facilitated by thermal energy. Consequently, this process is expected to be temperature-sensitive. To check this hypothesis, O_2 evolution under the 716 and 740 nm far-red light was measured at different temperatures.

In red light, the quantum yield of PSII tended to decrease at higher temperatures, while in the far-red light, there was a gradual increase of the quantum yield over the applied range of temperatures (Fig. 6A). Reasons of the quantum yield drop at temperatures over 30° were not investigated in this work. We assumed that, whatever reasons, they affected the quantum yield similarly under both red and far-red lights. Therefore, only the ratio of the yields was analyzed here.

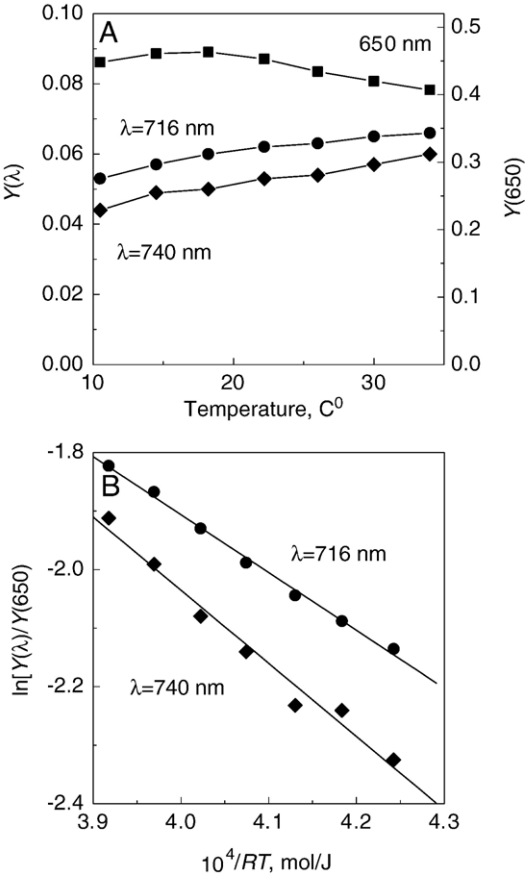

Fig. 6. Temperature dependencies of quantum yields at 716 and 740 nm in a sunflower leaf (panel A) and the Arrhenius plot of the ratio of the quantum yields at the two wavelengths (panel B), revealing activation energies of 9.8 and 12.5 kJ mol^{-1} at 716 and 740 nm, respectively. The background CO_2 and O_2 concentrations were 460 and 50 μmol mol^{-1}, respectively; the light intensities (incident/absorbed, μmol quanta m^{-2} s^{-1}) were 32/27 at 650 nm, 101/39 at 716 nm, and 215/11 at 740 nm. *RT* is the universal gas constant multiplied by absolute temperature.

The Arrhenius plot of quantum yield ratios, $Y(716)/Y(650)$ and $Y(740)/Y(650)$, is shown in Fig. 6B. The plot reveals the uphill activation energy of 9.8 ± 0.5 kJ mol^{-1} for 716 nm and 12.5 ± 0.7 kJ mol for 740 nm, comparable to the calculated energy gaps of 8.8 kJ mol^{-1} between the 716 and 680 nm and 14.3 kJ mol^{-1} between the 740 and 680 nm light quanta. This result confirms the assumed thermal activation of far-red light quanta to the PSII core.

3.6. Non-photochemical quenching of far-red excitations of photosystem II

Apart from the photochemical reaction, a non-photochemical quencher NPQ induced by excess light can also put out the PSII antenna excitations. In the following, we investigated whether the far-red PSII excitations could be quenched non-photochemically. The idea of the experiment was to evaluate the effect of NPQ on the oxygen evolution rate under red and far-red light.

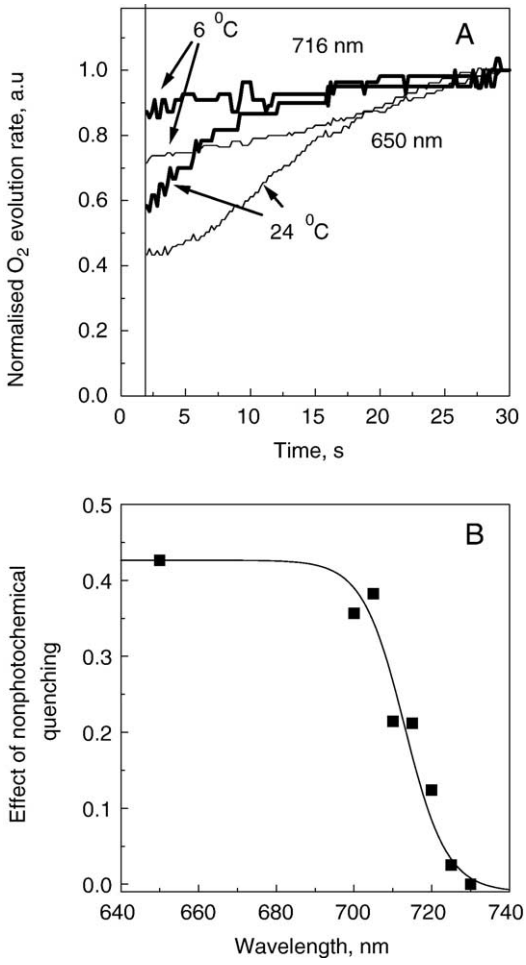

Fig. 7. Transients in oxygen evolution from a sunflower leaf due to the relaxation of non-photochemical quenching measured under 650 (thin lines) and 716 (thick lines) nm light at 6 and 24 °C (Panel A). Non-photochemical quenching was induced during a previous 2.5 min exposure under white light of 2200 μmol quanta m^{-2} s^{-1}. At time=0, the white light was replaced by the 650 or 716 nm low-intensity light (the absorbed light intensities were 27 and 39 μmol quanta m^{-2} s^{-1} at 650 and 716 nm, respectively). The recordings of O_2 evolution begin after 2 s from the switching the light sources (apparatus response cut off). Panel B: spectral dependence of NPQ measured at 22 °C, presented as $A_{30}/A_2 - 1$ (subscripts indicate the time of measurement of O_2 evolution A).

A sunflower leaf was pre-conditioned during 2.5 min under saturating white light of 2200 μmol quanta m^{-2} s^{-1} known to be inducing NPQ. Upon turning off the white light (at time zero, Fig. 7A), the recovering transients of O_2 evolution due to the relaxation of NPQ were recorded under the red and far-red light. At the ambient temperature, the 650-nm excitations were strongly quenched by NPQ induced under the strong white light. The quantum yield of O_2 evolution was decreased by about 50% of the value reached after the relaxation of the quencher during 30 s. The 716 nm far-red excitations were also quenched, but less than the red light excitations. Also, the kinetics of NPQ relaxation was faster when measured at 716 nm, compared to the 650 nm light. This drop of NPQ efficiency toward longer far-red was systematic, as Fig. 7B evidences. The differences for the red and far-red light were further amplified by low temperature, although then NPQ itself was generally lower. These results demonstrate that (i) the far-red excitations of PSII are susceptible to NPQ, but less than the red excitations, and (ii) NPQ of the far-red excitation is facilitated by temperature.

The origin of the spectral variations of NPQ deserves a special study. It is commonly assumed that NPQ occurs relatively far from the PSII reaction centre, in LHCIIb and/or in minor CP24, CP26, CP29 antenna complexes [15]. Our data may indicate that there is a correlation between spatial and spectral coordinates in the PSII antenna system. Excitations at different wavelengths then hit diverse complexes at different locations.

4. Discussion

We have found that quanta up to 780 nm wavelength induced O_2 evolution from the sunflower and bean leaves. This O_2 evolution was a result of the photochemical activity of PSII because excitation by the far-red light caused a parallel increase in Chl fluorescence, just like the excitation with shorter wavelength red light.

There are in principle several possibilities for the far-red light quanta to reach the PSII core and drive the photochemistry, including direct absorption in as yet undiscovered far-red Chls of the PSII antenna, reversed spill-over from the PSI antenna, and/or absorption from thermally populated vibrational sub-levels of PSII chlorophylls in the ground electronic state. In the following, we shall discuss these options.

4.1. Far-red chlorophylls in the photosystem II antenna

Our quantum yield value at 720 nm agrees well with the yield for O_2 evolution in *Chlorella* [1]. The spectral shape

of the PSII activity in the far-red, distinct from the leaf absorptance spectrum (Figs. 2 and 5), indicates that Chls responsible for the O_2 evolution should be minor relative to the Chls causing the bulk absorption in this region. Indeed, the yield of 0.07 would mean that less than 9% of absorbed far-red light quanta are effectively used to excite PSII. The rest, 91%, are then delivered to PSI. In getting these figures, we have assumed that the typical value of the quantum yield of excitation transfer to the reaction centre indicated by the variable fluorescence, $1-F_0/F_m=0.8$, holds also true for the far-red excitation. The combined absorption cross-section of the far-red Chls in the PSI antenna system corresponds to about 10 Chls [16]. Assuming similar absorption cross-sections for Chls in PSI and PSII, on average about one far-red Chl in each PSII may be present. This is in agreement with the result that O_2 evolution per saturating single turnover flash is about equal at flashing wavelength of 695 and 723 nm [6]. However, this is the upper limit. As the leaf absorbance at the local O_2 evolution yield maximum corresponds to a single PSI chlorophyll, rather than ten, the real figure may be smaller, making it very difficult, if not impossible, to detect these minor far-red PSII Chls using biochemical methods.

The literature evidence of red/far-red Chls in the antenna system of PSII is scarce [17–22]. In isolated CP43 and CP47 complexes, the redmost absorption bands are at 682 and 690 nm, respectively [17,19]. There are no observations of far-red absorption in those complexes. This is different from the peripheral LHCII antenna trimers where in a few cases a long-wavelength tail of the absorption spectrum up to 720 nm has been observed at room temperature [21,22]. The absorption spectra of more intact grana membrane fractions have demonstrated even further tailing reaching 740 nm [18]. Although an old question about possible influence of extraction procedures on spectral properties of antenna Chls may be revived at this point, one has to conclude that there is so far no physical evidence for the presence of longer than 740 nm absorbing PSII forms.

In intact leaves both PSII and PSI contribute in the long-wavelength emission. According to a recent analysis on barley leaves [23], at room temperature, most of the long-wavelength fluorescence at 750 nm in the F_m state with PSII reaction centres closed is emitted by PSII and only less than 10% by PSI. In the F_0 state with reaction centres open, the relative contribution of the PSI fluorescence is larger, being 10% at 680 nm and 50% at 820 nm. The plant fluorescence at ambient temperature is thus always dominated by PSII.

The in vivo Chl fluorescence spectrum generally contains two parts, which can be loosely classified as resonant and sideband components. For example, LHCII preparations from spinach, which show no absorption beyond 700 nm, show at 77 K a relatively narrow and intense resonant fluorescence band at 680 nm along with a broad and weak sideband peaking at 740 nm [24]. In optically thick samples, the ratio of the band amplitudes may change in favour of the sideband because of fluorescence reabsorption. For instance, in optically thin samples of chloroplasts and *Chlorella* at room temperature, the fluorescence emission at 740 nm constitutes about 18% of the peak height of the emission at 685 nm [7,25]. In intact leaves, the relative intensity of the 685 and 740 nm bands decreases with increasing Chl content until about equal intensity of the two peaks in fully developed green leaves is achieved [26]. It is therefore difficult to distinguish whether the long-wavelength fluorescence is a vibrational sideband of the bulk electronic transitions, enhanced due to reabsorption effect, or there is a component in it that is emitted by a minute number of far-red Chls in the PSII antenna. In the literature at least, the long-wavelength fluorescence emission of PSII constituents has always been ascribed to the vibrational sideband [7]. However, the presence, at −196 °C, of a local emission maximum at 750 nm in PSII fluorescence, but not in LHC fluorescence in bean leaves [27], is speaking against the vibrational sideband and indicates the presence of a small number of special far-red Chls in the PSII core.

4.2. Reversed spill-over

A possibility of energy transfer energetically downhill from PSII to PSI antenna, termed spill-over [27–29], has been proposed to have importance in regulating the excitation distribution between the photosystems. It has also been suggested [30,31] that the far-red Chl excitations of the PSI antenna may be transferred to the PSII antenna by reversed spill-over. The major problem with the latter model is a requirement of a tight contact between the PSI and PSII antennae. Also, relatively long lifetime of far-red PSI excitations is necessary for such energetically uphill transfer of excitations.

The domain organization of plant thylakoid membrane implies that the two photosystems are spatially segregated, the PSI being enriched in the stroma thylakoids and the peripheral part of the grana thylakoids, while PSII dominating in the central part of the grana [32]. Rearrangements in the PSII and PSI antenna have been implicated in the so-called state 1 to state 2 transitions, another mechanism which regulates the light energy distribution between the two photosystems [33,34]. The state 1 (conversely state 2) can loosely be defined as a state of adaptation of the plant photosynthetic machinery to the light that is predominately absorbed by PSI (PSII) complexes. In state 1, the prime concern of this work, the connectivity of the complexes is decreased [33], making the reversed spill-over mechanisms highly unlikely. Moreover, we most probably miss in our samples not only the reversed spill-over, but also the significant direct spill-over. If the probability of the reverse spill-over was 9%, then the probability of the direct spill-over had to be much higher. Such a high rate of energy flow from PSII to PSI would leave no room and importance for the regulation by state transition, which is estimated to involve about 10% of the bulk PSII antenna [35]. In our experiment of Fig. 4, the quantum yield for the 650-nm light

decreased by 25% after the far-red light was switched off, which could reflect the movement of +12.5% Chl to PSII, leaving PSI underexcited by −12.5%. A concomitant increase of the fluorescence was observed, being a clear demonstration of over-excitation of PSII, but after a while, the excitations of the two photosystems became balanced again, evidently due to the state 1→ state 2 transition. Thus, even if the initial increase of fluorescence was accompanied by spill-over, in steady state, the photosystems were balanced by the state transition mechanism. Since the direct spill-over was not able to balance excitations between the photosystems, the significance of the reverse spill-over was most probably minor.

As for the long lifetime of the far-red PSI pigments required for effective reversed spill-over, it is not supported by the experiment either. Uphill thermal activation of excitations from the far-red states of PSI to the bulk PSI antenna and their subsequent photochemical trapping in the PSI centre is well established [36]. The uphill character of the process slows down the overall energy flow from the antenna to the reaction centre, however, not to the extent that would significantly decrease the quantum efficiency of the primary energy trapping in PSI [36]. The PSI trapping time, which increases across the far-red absorption tail varying between 81 and 103 ps at 280K [36], is considerably shorter than the PSII lifetime of 300–600 ps measured in intact cells of green algae [37]. Moreover, since the transfer time from the far-red Chls to the 680 nm reaction centre trap of PSII must be longer than for the 700 nm reaction centre trap of PSI, the competition by the 700 nm trap must become increasingly dominating with increasing wavelength. This was not observed. On the contrary, as seen in Figs. 2 and 5, the quantum yield of O_2 evolution was increasing in a relatively wide wavelength range between 710 and 750 nm.

Generally speaking, if the rate constant of the direct spill-over is so slow that significant excitation transfer to PSI can occur only from the long-living high-fluorescent (F_m) state of PSII, then the probability for uphill excitation transfer from the short-living low-fluorescence (F_0) state of PSI must be minute.

4.3. Absorption from thermally populated vibrational sub-levels of photosystem II chlorophylls

The third possibility to interpret our observations is optical excitation from thermally populated high-energy vibrational sub-levels of the PSII Chls in the ground electronic state. The optical energy needed to cover the gap between the ground and excited electronic states is then reduced by the energy of vibrational quanta. This interpretation is inspired by the observed thermal activation of the O_2 evolution (Fig. 6) as well as by similar location around 745 nm of the peaks in the quantum yield spectrum (Figs. 2 and 5) and vibrational sidebands in the fluorescence spectra of PSII constituents (see, e.g., [24,38]).

Multiple vibrations generally contribute into the vibrational sideband of optical spectra. Yet, in many cases, it is reasonable to consider just a single vibrational mode, the one most strongly coupled to the electronic transition and responsible for the maximum of the fluorescence/absorption sideband. Here, we take the effective vibrational frequency equal to 1225 cm^{-1} (~14.7 kJ mol^{-1}), being characteristic to the LHCII complex [24,38]. The relative population of the first excited and ground state levels of that vibration at ambient temperature, calculated as the Boltzmann factor, is $e^{-6} \approx 1/410$. To get the relative absorbance from the excited vibrational state with respect to that from the ground state, this ratio should further be reduced by a factor of 7–8 [38] because of smaller overlap of excited and ground state vibrational wave-functions. The expected absorbance of PSII Chls at 745 nm is thus about 3000-fold weaker than that at 680 nm. This figure should be compared with the one deduced from absorptance and quantum yield data.

Based on the experimental absorptance spectrum the absorbance (optical density) spectrum of the leaf, $A(\lambda)$, can be calculated as

$$A(\lambda) = -lg[1 - a(\lambda)]. \quad (2)$$

From the data of Fig. 5, considering maximum reflectance of about 0.05 at 680 nm, the so calculated absorbance (optical density) ratio A(680)/A(745) is about 70. According to our previous estimates up to 9% of the quanta absorbed at 745 nm end up on PSII pigments. Assuming that the corresponding figure at 680 nm is 50%, the ratio of optical densities of PSII Chls at 680 and 745 nm is about 350. This estimate is still much smaller than the anticipated number of 3000 for this mechanism. It is difficult to imagine how these two estimates could be brought into reasonable agreement without dubious adjustment of the parameters, even considering all the difficulties of measuring highly light scattering and optically thick leaf.

5. Conclusions

From the three interpretations discussed, we favour the first one, i.e., the presence of far-red PSII Chls in intact plant leaves, so far unrecognized. This explanation also seems natural taking the shape of the quantum yield spectrum. However, one should be careful here. The quantum yield spectrum calculated according to Eq. (1) does not provide direct information about absorption spectra of the species active in photochemistry. This is because several overlapping spectral forms belonging both to PSII and PSI are contributing into the absorptance spectrum that appears in the denominator of Eq. (1). The quantum yield therefore reflects the changing relative input of all spectral forms, rather than the absorption spectrum of any single PSII contributor. The similarity of the result for sunflower and bean proves that both the extreme long-wavelength oxygen evolution and the local quantum yield maximum are general

properties of plants. Clearly, more work should be done to meet the challenges brought up by this investigation. One of them would be the origin of long-wavelength Chls. Unfortunately, a small number of the pigments makes it very difficult to prove or disprove our hypothesis using traditional analytical methods, as the weakly bound pigments may be easily lost. From the physical point of view and relying on analogy with the far-red spectral forms in green plant PSI (see [39] and references therein), to produce such a large red shift, it is likely that some kind of strongly coupled Chl dimers/aggregates are involved.

Acknowledgements

The Estonian Science Foundation (Grants No. 5236 and 5543) and the Hasselblad Foundation have supported this work. We thank M. Rätsep for the help with the laser system. We also appreciate useful comments from professor-emer. Govindjee and the personal communication by professor-emer. U. Heber that far-red excitations increase the PSII fluorescence in a desiccated poikilohydric fern *Polypodium vulgare*, received after this work was completed.

References

[1] R. Emerson, C.M. Lewis, The dependence of quantum yield of *Chlorella* photosynthesis on wavelength of light, Am. J. Bot. 30 (1943) 165–178.
[2] R. Emerson, C.M. Lewis, Factors influencing the efficiency of photosynthesis, Am. J. Bot. 26 (1943) 808–822.
[3] R. Emerson, R.V. Chalmers, C.N. Cederstrand, Some factors influencing the longwave limit of photosynthesis, Proc. Natl. Acad. Sci. U. S. A. 43 (1957) 133–143.
[4] J. Myers, J.-R. Graham, Enhancement in *Chlorella*, Plant Physiol. 38 (1963) 105–116.
[5] B. Gobets, R. van Grondelle, Energy transfer and trapping in photosystem I, Biochim. Biophys. Acta 1507 (2001) 80–99.
[6] N.L. Greenbaum, D. Mauzerall, Effect of irradiance level on distribution of chlorophylls between PSII and PSI as determined from optical cross-sections, Biochim. Biophys. Acta 1057 (1991) 195–207.
[7] E. Rabinowitch, Govindjee, Photosynthesis, John Wiley & Sons, Inc., New York, 1969.
[8] D. Mauzerall, N.L. Greenbaum, The absolute size of a photosynthetic unit, Biochim. Biophys. Acta 974 (1989) 119–140.
[9] Govindjee, On the requirement of minimum number of four versus eight quanta of light for the evolution of one molecule oxygen in photosynthesis: a historical note, Photosynth. Res. 59 (1999) 249–254.
[10] E. Greenbaum, D.C. Mauzerall, Oxygen yield per flash of *Chlorella* coupled to chemical oxidants under anaerobic conditions, Photochem. Photobiol. 23 (1976) 369–372.
[11] H. Pettai, V. Oja, A. Freiberg, A. Laisk, The long wavelength limit of plant photosynthesis, FEBS Lett. (2005).
[12] V. Oja, H. Eichelmann, R.B. Peterson, B. Rasulov, A. Laisk, Deciphering the 820 nm signal: redox state of donor side and quantum yield of photosystem I in leaves, Photosynth. Res. 78 (2003) 1–15.
[13] A. Laisk, V. Oja, B. Rasulov, H. Rämma, H. Eichelmann, I. Kasparova, H. Pettai, E. Padu, E. Vapaavuori, A computer-operated routine of gas exchange and optical measurements to diagnose photosynthetic apparatus in leaves, Plant Cell Environ. 25 (2002) 923–943.
[14] B. Diner, D. Mauzerall, Feedback controlling oxygen production in a cross-reaction between two photosystems in photosynthesis, Biochim. Biophys. Acta 305 (1973) 329–352.
[15] P. Horton, A.V. Ruban, M. Wenworth, Allosteric regulation of the light-harvesting system of photosystem II, Philos. Trans. R. Soc. Lond., B 355 (2000) 1361–1370.
[16] R. Croce, G. Zucchelli, F.M. Garlaschi, R. Bassi, R.C. Jennings, Excited state equilibration in the photosystem I-light-harvesting I complex: P700 is almost isoenergetic with its antenna, Biochemistry 35 (1996) 8572–8579.
[17] H.C. Chang, R. Jankowiak, C.F. Yocum, R. Picorel, M. Alfonso, M. Seibert, G.J. Small, Exciton level structure and dynamics in the CP47 antenna complex of photosystem II, J. Phys. Chem. 98 (1994) 7717–7724.
[18] F.L. de Weerd, M.A. Palacios, E.G. Andrizhiyevskaya, J.P. Dekker, R. van Grondelle, Identifying the lowest electronic states of the chlorophylls in the CP47 core antenna protein of photosystem II, Biochemistry 41 (2002) 15224–15233.
[19] F.L. de Weerd, I.H.M. van Stokkum, H. van Amerongen, J.P. Dekker, R. van Grondelle, Pathways for energy transfer in the core light-harvesting complexes CP43 and CP47 of photosystem II, Biophys. J. 82 (2002) 1586–1597.
[20] R.C. Ford, S.S. Stoylova, A. Holzenburg, An alternative model for light-harvesting complex II in grana membranes based on cryo-electron microscopy studies, Eur. J. Biochem. 269 (2002) 326–336.
[21] S.L.S. Kwa, H. van Amerongen, S. Lin, J.P. Dekker, R. van Grondelle, W.S. Struve, Ultrafast energy transfer in LHC-II trimers from the Chl a/b light-harvesting antenna of photosystem II, Biochim. Biophys. Acta 1102 (1992) 202–212.
[22] G. Zucchelli, R.C. Jennings, F.M. Garlaschi, The presence of long-wavelength chlorophyll *a* spectral forms in the light-harvesting chlorophyll *a/b* protein complex II, J. Photochem. Photobiol., B 6 (1990) 381–394.
[23] F. Franck, P. Juneau, R. Popovic, Resolution of the photosystem I and photosystem II contributions to chlorophyll fluorescence of intact leaves at room temperature, Biochim. Biophys. Acta 1556 (2002) 239–246.
[24] H. Kirchhoff, J. Hinz, J. Rösgen, Aggregation and fluorescence quenching of chlorophyll *a* of the light-harvesting complex II from spinach *in vitro*, Biochim. Biophys. Acta 1606 (2003) 105–116.
[25] Govindjee, L. Young, Structure of the red fluorescence band in chloroplasts, J. Gen. Physiol. 49 (1966) 763–786.
[26] H.K. Lichtenthaler, Laser-induced chlorophyll fluorescence of living plants, Proceedings of the IGARSS' 86 Symposium, 8–11 Sept. 1986, Zürich, ESA SP-254 ESA Publication Division, 1986, pp. 1571–1579.
[27] W.L. Butler, Energy distribution in the photochemical apparatus of photosynthesis, Annu. Rev. Plant Physiol. 29 (1978) 345–378.
[28] K. Satoh, R. Strasser, W.L. Butler, A demonstration of energy transfer from photosystem II to photosystem I in chloroplasts, Biochim. Biophys. Acta 440 (1976) 337–345.
[29] M. Mimuro, N. Tamai, T. Ishimaru, I. Yamazaki, Characteristic fluorescence components in photosynthetic pigment system of a marine dinoflagellate, *Protogonyaulax tamarensis*, and excitation anergy flow among them. Studies by means of steady-state and time-resolved fluorescence spectroscopy, Biochim. Biophys. Acta 1016 (1990) 280–287.
[30] R.J. Jennings, G. Forty, Evidence for energy migration from photosystem I to photosystem II and the effect of magnesium, Biochim. Biophys. Acta 376 (1975) 89–96.
[31] B. Koehne, G. Elli, R.C. Jennings, C. Wilhelm, H.-W. Trissl, Spectroscopic and molecular characterization of a long wavelength absorbing antenna of *Ostreobium sp*, Biochim. Biophys. Acta 1412 (1999) 94–107.

[32] P.-A. Albertsson, A quantitative model of the domain structure of the photosynthetic membrane, Trends Plant Sci. 6 (2001) 349–354.
[33] J.F. Allen, J. Forsberg, Molecular recognition in thylakoid structure and function, Trends Plant Sci. 6 (2001) 317–326.
[34] J. Zhao, G. Shen, D.A. Bryant, Photosystem stoichiometry and state transitions in a mutant of the cyanobacterium *Synechococcus* sp. PCC 7002 lacking phycocyanin, Biochim. Biophys. Acta 1505 (2001) 248–257.
[35] J.F. Allen, T. Pfannschmidt, Balancing the two photosystems: photosynthetic electron transfer governs transcription of reaction centre genes in chloroplasts, Philos. Trans. R. Soc. Lond., B 355 (2000) 1351–1360.
[36] R.C. Jennings, G. Zucchelli, R. Croce, F.M. Garlaschi, The photochemical trapping rate from red spectral states in PSI-LHCI is determined by thermal activation of energy transfer to bulk chlorophylls, Biochim. Biophys. Acta 1557 (2003) 91–98.
[37] J. Wendler, A.R. Holzwarth, State transitions in the green alga *Scenedesmus obliquus* probed by time-resolved chlorophyll fluorescence spectroscopy and global data analysis, Biophys. J. 52 (1987) 717–728.
[38] J. Pieper, R. Schödel, K.-D. Irrgang, J. Voight, G. Renger, Electron-phonon coupling in solubilized LHCII complexes of green plants investigated by line-narrowing and temperature-dependent fluorescence spectroscopy, J. Phys. Chem. B 105 (2001) 7115–7124.
[39] J.A. Ihalainen, M. Rätsep, P.E. Jensen, H.V. Scheller, R. Croce, R. Bassi, J.E.I. Korppi-Tommola, A. Freiberg, Red spectral forms of chlorophylls in green plant PSI. A site-selective spectroscopy study, J. Phys. Chem. B 107 (2003) 9086–9093.